Adsorptive Removal of Crystal violet (CV), a Carcinogenic Textile Dye, from Aqueous Solution by Conducting Polyaniline/ Hollow Manganese Ferrite Nanocomposites

Rahmatollah Rahimi [a], Hamed Kerdari [b], Mahboubeh Rabbani[a]

Rahimi_rah@iust.ac.ir

[a] Chemistry Department, Iran University of Science and Technology, Tehran, Iran

[b] Chemistry Department, Islamic Azad University, Saveh Branch, Saveh, Iran

Abstract:

The conducting protonated polyaniline/ hollow $MnFe_2O_4$ nanocomposite was successfully synthesized in situ through self assembly polymerization. The core-shell of $MnFe_2O_4$ hollow spheres were fabricated by template polymerization, at first, the ferrite nanoparticles were synthesized as the shell and coated on the surface of functionalized polystyrene spheres as the core, subsequently, by calcination method the core polymer was removed. The ferrite nanoparticles were combined with PANI by assisting of dodecyl benzene sulfonic acid as doping agent under ultrasonic waves. The difference between the spectra of FT-IR for the ferrite nanoparticles-coated PS spheres and $MnFe_2O_4$ hollow spheres show the elimination of organic template after calcinations. The image of scanning electron microscopy (SEM) exhibit the ferrite spheres as nanoporous with size holes of 40 nm approximately. Also the magnetic properties of the nanocomposite and $MnFe_2O_4$ were characterized on a vibrant sample magnetometer (VSM) with maximum saturation magnetization values of 1.59 emu/g and 66.7 emu/g respectively. X-ray diffraction (XRD) pattern of the ferrite sample is well in agreement with the standard pattern of the cubic structure. Atomic force microscopy (AFM) was used for surface morphology analysis. UV–Visible absorption spectroscopy recorded the adsorption behavior of the solution after treatment with synthesized nanocomposite showing the adsorption capacity of Crystal violet dye.

Keywords: "Polyaniline; Hollow ferrite; Surfactant; Adsorptive removal"

1. Introduction

Polyaniline (PANI) as a classic conducting polymer and the low cost of its monomer has been centre of great attention recently. It is known that PANI has a variety of oxidation states of which three of them are commonly referred to, in the literature [1–3]: leucoemeraldine base (LEB, fully reduced), emeraldine base (EB, half-oxidized) and pernigraniline base (PNB, fully oxidized). Therein, EB is the most attractive one, because it can be doped with protonic acid to become emeraldine salt (ES) and the DC conductivity of the ES is increased due to the charge delocalization on the polymer backbone created by doping H^+. Conducting polymer composites with micro/nanostructures have attracted significant academic and technological attention because of their unique physical properties and potential applications in nanoelectronics, electromagnetics, and biomedical devices [4]. Among these conducting polymer composites, materials decorated with inorganic nanoparticles are of particular interest because possible interactions between the inorganic nanoparticles and the polymer matrices may generate some unique physical properties upon the formation of various micro/nanocomposites[5-8]. In recent years, composites containing PANI and magnetic oxides exhibiting different nanostructures, such as nano-tubes, nanorods, or core-shell nanostructures, have been extensively studied [9-12] but their investigation on hollow or porous composites were seldom reported. Hollow inorganic spheres represent a special class of materials, which are of interest in the fields of medicine, pharmaceuticals, materials science, and the paint industry. In particular, the low densities of the hollow spheres are expected to increase the stability of suspensions when compared to their solid counterparts. This characteristic is highly advantageous for separation applications. Furthermore, there is growing interest in magnetic hollow spheres, which have remarkable application advantages in biomedicine especially in target drug delivery because of its magnetic properties and hollow structure. Strategies to produce magnetic hollow spheres are mainly based on the sequential adsorption (layer-by-layer self assembly) of magnetic nanoparticles onto colloidal templates, normally silica or polystyrene (PS) spherical particles, and the further removal of the core either with the addition of a solvent or high temperature [13-14]. Color is the first contaminant to be recognized in wastewater. Dyes are used in different industries such as paper and plastics, leather, pharmaceutical, food, cosmetics, dyestuffs, textiles, etc. to color the products. As a result, considerable amount of colored wastewater is generated. The presence of these dyes in water even at very low concentration is highly visible and undesirable [15]. A wide range of methods have been developed for the removal of synthetic dyes from waters and wastewaters to decrease their impact in environment. Among these physico-chemical methods like adsorption [16-17], electrochemical coagulation [18] are popular now. Adsorption is one of the methods, which is obtaining more attention because of its easy operations and versatility. It is a useful and simple technique and allows kinetic and equilibrium measurements without any highly complicated instruments [19]. In the present paper polyaniline/ hollow $MnFe_2O_4$ nanocomposite was employed for removal of CV and used as an adsorbent in the wastewater treatment. The technique was found to be useful and cost-effective for a removal of dye.

2. Experimental

Materials and Instrumentals

The monomers of aniline (Merck), styrene (Merck) were vacuum-distilled to remove the inhibitor prior to use; Acrylic acid (Aldrich, analytical purity) was used as received. Other chemicals including metal salts, ethylene glycol (EG), potassium persulfate (KPS), Ammonium persulfate (APS), Hexamethylene tetraamine (HMTA), potassium nitrate, dodecyl benzene sulfonic acid (DBSA) and Crystal violet (CV) dye were generally reagent grade from commercial sources and used without further purification. Water was deionized and deoxygenated prior to use.

The morphology of the particles was examinated by scanning electron microscopy (SEM, Vega II model, Tescan). Fourier transform infrared spectroscopy (FTIR) spectra were recorded on a PerkinElmer spectrum FTIR using KBr pellets. Atomic force microscopy (AFM, Nano Scope II from digital Instruments Inc., CA, USA in contact mode) was used for surface morphology analysis of composite. Hollow particles of ferrite were examined by X-ray diffraction (XRD, Japan Jeol JDX-8030, operated at 30 kV and 20 mA). A vibrating-sample magnetometer (VSM, Lakeshore) was used to study the magnetic properties of ferrite particles and composite. Conductivity changes were measured with four-probe device (ASTM Standards, F 43-93). UV–Visible absorption spectroscopy (Shimadzu- 1700 model, pharmaspec) was used to inscribe of adsorption behavior. pH meter (Metrohm AG, CH-9101 Herisau, Switzerland) was used to gain various pHs.

2.1. Experimental procedure

2.1.1. Synthesis of polystyrene-acrylic acid copolymer

Negatively charged PS spheres which were used as core particles, were prepared by a free–emulsion polymerization method, generally 5 ml of styrene (0.044 mol), 1 ml of acrylic acid (0.015 mol) were added to the flask with 50 ml deionized water. To eliminate oxygen effects, the solution was purified with nitrogen for 15 minutes under gentle stirring then process was initiated by adding 0.03 g KPS. The mixture was heated to 72˚C under nitrogen stirring with a magnetic stirrer. After 24 hr, the mixture was cooled to room temperature and the colloidal solution of functionalized PS spheres was prepared.

2.1.2 Coated particles

In a typical process, 4 ml PS colloid solution was diluted 400 ml deoxygenated distilled water and then mixed with 100 ml of metal salts solution which included 3.98 gr. $Fecl_2.4H_2O$ (0.02 mol) and 1.62 gr. $MnCl_2.2H_2O$ (0.01 mol) and was agitated for 5 minutes, then flask was placed in ultrasonic system for 10 minutes, then 10 ml EG was poured in reaction solution and was dispersed for excess 15minutes by ultrasonic, the mixture was incorporated with 8 gr. HMTA and 1gr potassium nitrate. Flask was heated to 85 ˚C immediately under gentle stirring. The mixture color changed to black-brown gradually. After 3 hr, system was cooled to room temperature and was poured into excess distilled water then magnetic particles were deposited by magnetic field. The precipitate was washed with distilled water for several times and then dried in oven at 70˚C for 12 hr. the dried residue was grinded to improve calcination process.

2.1.3 Hollow ferrite spheres

Hollow ferrite nanoparticles were produced as the particles calcined for 3 hr under nitrogen atmosphere at 500˚C [20].
The heating rate was 10˚C min^{-1} below 150˚C and 5 ˚C min^{-1} between 150˚C to 500˚C.

2.1.4 Synthesis of PANI/hollow Mn-Fe_2O_4 nanocomposite

4 ml aniline (0.044 mol) and 10 ml distilled water were mixed and agitated for 15 min, in another container 5gr dodecyl benzene sulfonic acid (DBSA) was diluted with 10ml of deionized water to form pulpy mixture, and then solution was poured into prepared solution of aqueous aniline, this emulsion was entirely stirred for 1 hr by magnetic stirrer to form homogenous phase.
In the next step 5 ml of aqueous solution containing 0.6 g of hollow ferrite spheres was placed in ultrasonic system for 10 minutes and added to above suspension, and mixture was again sonicated for an extra 15 minutes, and then was gently agitated by mechanical stirrer for an additional 15 min, 10 ml of an aqueous solution containing 5 g of APS (0.022 mol) as oxidizing agent was slowly added (during 15 min) while stirring mechanically to begin polymerization reaction. The resulting green precipitate (PANI/ hollow $Mnfe_2O_4$ nanocomposite) was filtered, washed with distilled water for two times and then dried overnight in an oven at 60˚C.

2.1.5 Adsorption of CV

Adsorption studies were performed by adding 0.05 g nanocomposite to the 50mL solution of different concentrations of CV in a beaker. The pH of the CV solution was adjusted at 7 using 0.01 mol L^{-1} HCl and 0.01 mol L^{-1} NaOH and the solution was agitated by mechanical stirrer for 15 min. Then CV loaded nanocomposite was separated with magnetic decantation and centrifugation at 3000 rpm for 5 min. The concentration of CV in the solution was measured spectrophotometrically at 590 nm. The concentration of CV decreased with time due to its adsorption by polyaniline/ hollow $MnFe_2O_4$ nanocomposite.

3. Result and Discussion

3.1. Material characterization

Figure.1 illustrates the FT-IR spectra of $MnFe_2O_4$ coated functionlized PS spheres

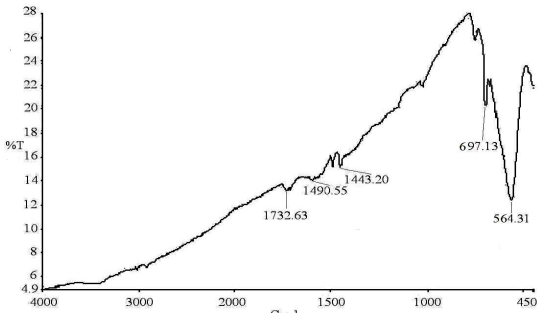

Fig.1 FT-IR spectra of the $MnFe_2O_4$ coated on PS spheres

The typical absorption peaks at 1443.20/1490.55, 697.13 cm^{-1} are attributed to benzene ring backbone mode in PS, the out of plane bending vibration mode of the mono subsituted benzene ring group of PS respectively, and the peak at 1732.63 cm^{-1} is a characteristic absorption of the vibration of C=O bond in acrylic acid, A wide band in the spectra of the coated PS spheres can be seen at ~3450 cm^{-1}, which is attributed to the hydroxyls groups in acrylic acid. The sharp peak at 564.31cm^{-1} is corresponded to the Fe–O stretching vibration of the ferrite.

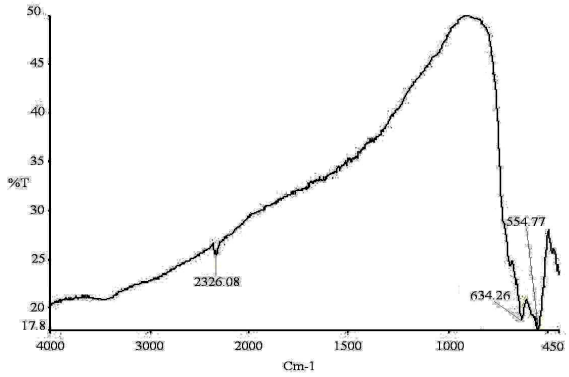

Fig.2 FT-IR spectra of ferrite hollow spheres calcined at 500 ° c

Figure.2 illustrates the FT-IR spectra of calcined hollow Mn-Fe_2O_4 nanoparticles. These picks at 697.13 cm^{-1}/~750 cm^{-1}, 1443.20/1490.55 cm^{-1} and 1732.63 cm^{-1} are related to the charged polystyrene which disappeared after calcinations at 500 ˚C and causing the hollow spheres. The peak at 554.77 cm^{-1} is sharpened after calcinations corresponding to the Fe–O stretching vibration of the ferrite.

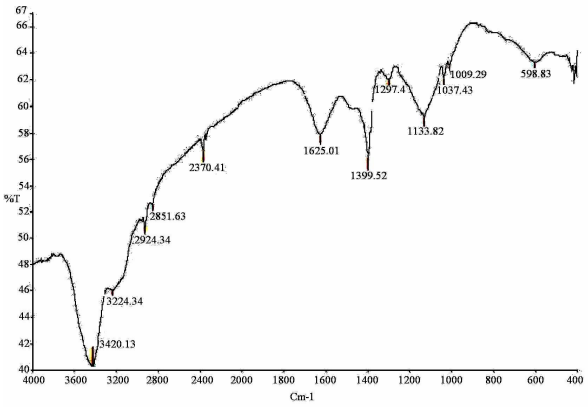

Fig.3 FT-IR spectra of PANI/ Hollow $MnFe_2O_4$ Nanocomposite

Fig.3 Shows the FT-IR spectra of PANI/hollow $MnFe_2O_4$ nanocomposite, the weak peak at ~505 cm^{-1} is attributed to SO_3H group of DBSA surfactant [21]. Absorption band at 598.83 cm^{-1} is corresponding to Fe-O stretching vibration. There are characteristic peaks of PANI-DBSA at 1133.82/1297.40, 1399.52/1625.01, 3420.13 cm^{-1} which are attributed to the C-N stretching vibration band, the C=C stretching vibration in the aromatic ring, the N-H bond vibration respectively, indicating the existence of the main chain structure of the conductive doped PANI in this composite [22].

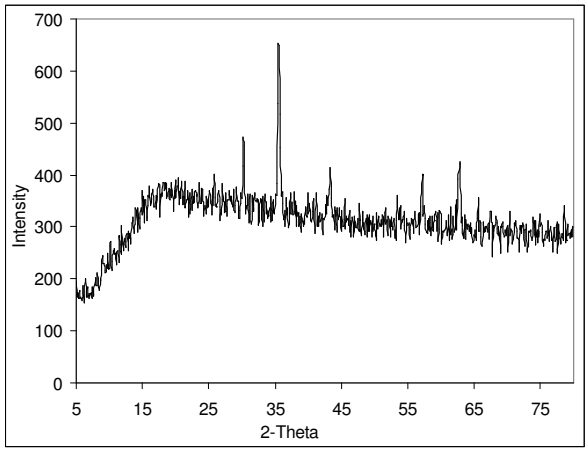

Figure.4 X-ray diffraction pattern of hollow Mn-Fe_2O_4

Fig.4 demonstrates the XRD pattern of the hollow ferrite spheres. The position and relative intensity of all diffraction peaks match well with those of Fe_3O_4 and Mn-Fe_2O_4 according to standard cards No.: 19-0629, 10-0319, 32-0637. While sharp peaks at 35.5˚, 30.2˚, 57.2˚, 62.9˚ are attributed to magnetite and weak peaks at 18.1˚, 43.3˚, 47.7˚ belongs to manganese ferrite. The presence of magnetite indicators are due to the lower molar percentage of manganese chloride in the reaction compared to iron chloride; Therefore the resulting compound is a mixture of Mn-Fe_2O_4 and magnetite. The device used is λ= 1.54 Å and β= 0.30˚ which is the equivalent of 0.005 radian. The average crystallite size of Mn-Fe_2O_4 particles was estimated by the scherer formula at 28.55 nanometers. Based on the results of the XRD curve and the mentioned standard patterns, Mn-Fe_2O_4 is expected to be in cubic system.

3.2 Morphology Analysis

A scanning electron microscopy (SEM) image of porous or hollow $MnFe_2O_4$ nanospheres is displayed in figure.5. As it can be seen, there are numerous uniform spherical particles containing holes in the center of some spheres with diameter of about 40 nm and the hollows were generated by removing organic template during calcinations process.

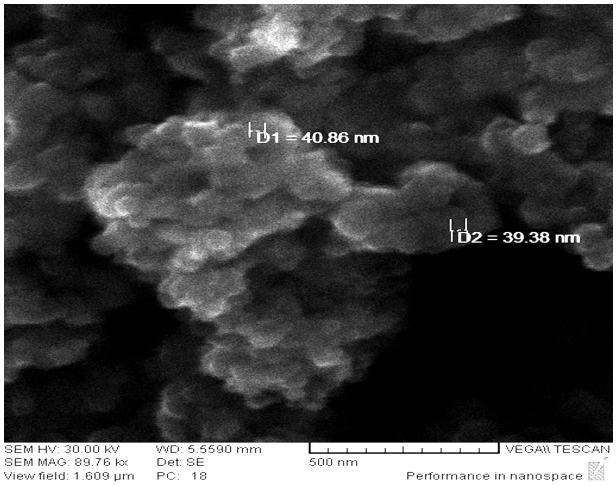

Figure.5 SEM image of hollow $MnFe_2O_4$ nanospheres.

Fig.6 shows the AFM image of surface structure as-prepared of PANI-DBSA/hollow Mn-Fe_2O_4 nanocomposite film containing 0.25 gr of nanocomposite dissolved in 5 ml NMP solution. Numerous bumps were seen of the surface of the composite as seen in the image, which indicates the presence of Mn-Fe_2O_4 magnetic nanoparticles in the polymer. Agglomerations can be seen in some areas which indicate the accumulation of magnetic particles resulting from much attraction between the nanoparticles.

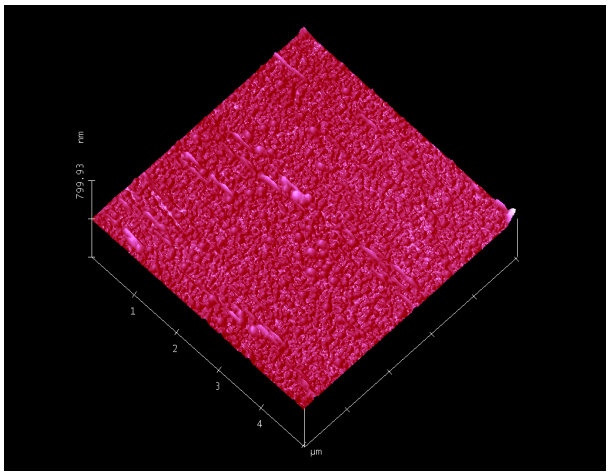

Figure.6 AFM image of surface PANI/hollow ferrite nanocomposite

Figure.7 the AFM image is of the top perspective of the nanocomposite which contains numerous dots. This indicates the even distribution of magnetic nanoparticles in the composite. The purple color indicates the size 200 nm for the composite accumulation.

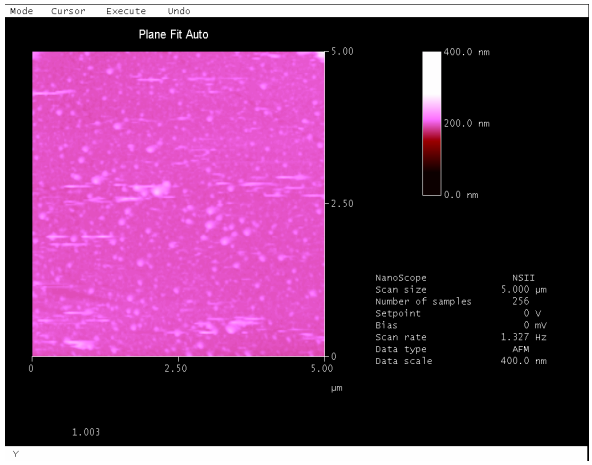

Figure.7 AFM image of the top surface PANI/ hollow ferrite nanocomposite

Figure.8 the AFM image indicates the height of Mn-Fe_2O_4 particles. According to the picture the height of nanoparticles were estimated at 23/655.

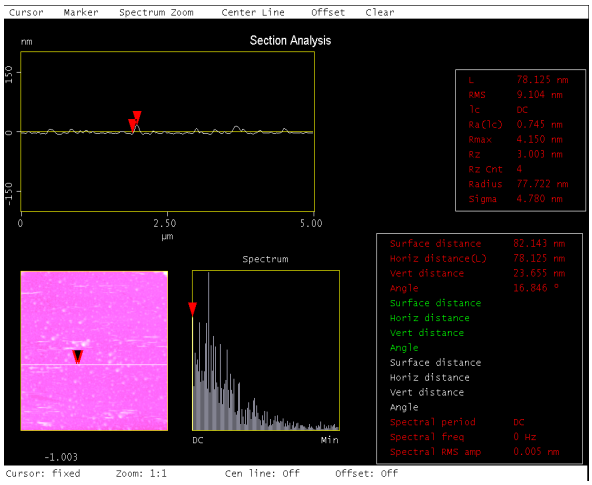

Figure.8 AFM image of the height of ferrite nanoparticles in PANI/ hollow ferrite nanocomposite

Figure.9 the AFM image indicates the width of Mn-Fe_2O_4 particles. According to the picture the width of nanoparticles were estimated at 175.78

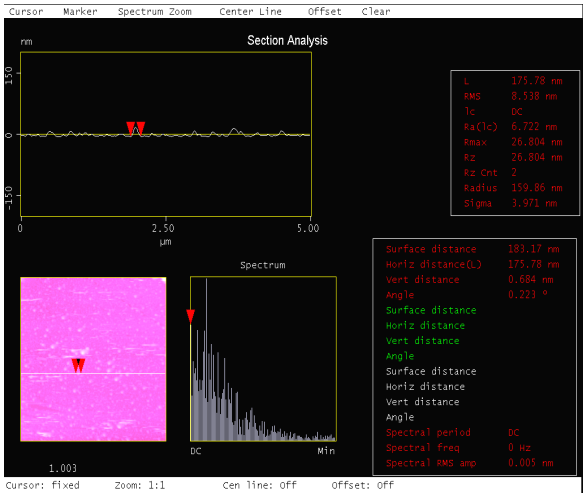

Figure.9 AFM image of the width of ferrite nanoparticles in PANI/ hollow ferrite nanocomposite

Figure.10 the AFM image indicates the roughness of PANI/hollow $MnFe_2O_4$ nanocomposite. According to the image, the maximum amount of unevenness in the composite surface is estimated at 94/927 nm.

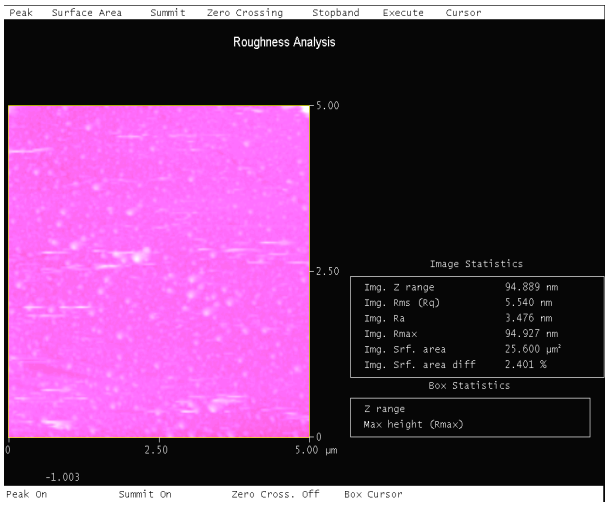

Figure.10 AFM image of the roughness of PANI/ hollow ferrite nanocomposite

3.3. Magnetic properties

The magnetic properties of the hollow ferrite were analyzed by room temperature VSM with an applied field -8.2≤H≤8.2 kOe field, the value of saturation magnetization (M_s) is about 66.7 emu/g, the remnant magnetization (M_r) and coercivity field are 17.81 emu/g and 110 Oe respectively.

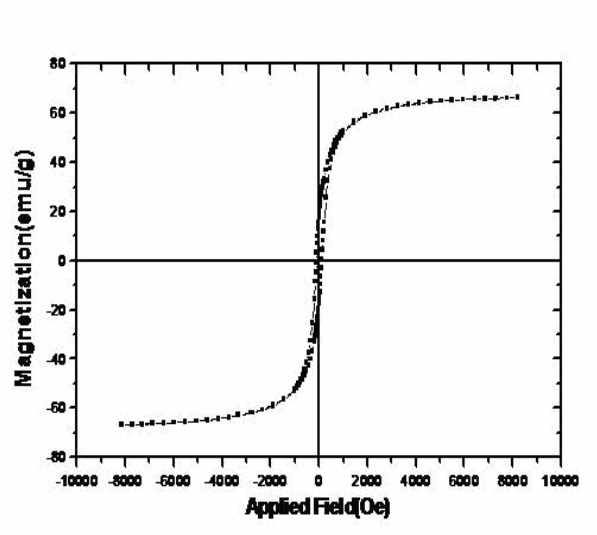

Figure.11 Magnetization curve of hollow ferrite

Figure.12 shows clear saturation between -8.2≤H≤8.2 kOe with saturation magnetization (M_s) about 1.59 emu/g and the remnant magnetization (M_r) about 0.35 emu/g for nanocomposite which is lower than pure manganese ferrite nanoparticles, so the magnetization curve of the sample shows weak ferromagnetic behavior, with slender hysteresis. Magnetic properties of nanocomposites containing magnetite or ferrite particles have been believed to be highly dependent on the sample shape, crystallinity, and the value of magnetic particles, so that they can be adjusted to obtain optimum property.

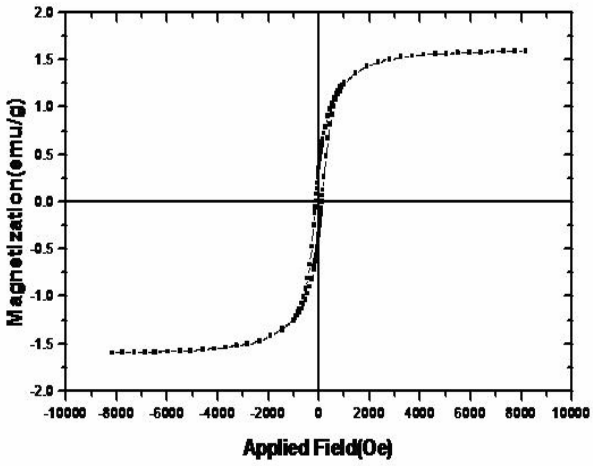

Figure.12 Magnetization curve of PANI/hollow $MnFe_2O_4$ nanocomposite

3.4. Conductivity properties

Conductivity of PANI/hollow $MnFe_2O_4$ nanocomposite doped with DBSA surfactant was assessed using four probe conductivity assessing device and the average of the assessments were at 1/10

S/cm. This reveals that acidic hydrogen of -SO3H group in DBSA has a well ability of doping the PANI.

3.5. Effect of pH

The effect of pH in the range 5–9 on the removal of CV was investigated using 0.01 mol L^{-1} HCl or NaOH solutions for pH adjustment, with the initial CV concentration fixed at 5 ppm. As Fig. 12 shows, the percent adsorption increased by raising of pH and reached maximum (75.6%) at pH 7 and then decreased at higher pHs. Generally at higher pHs, the amine sites of polyaniline chain were deprotonated and polyaniline did not prefer the adsorption of CV due to electrostatic repulsion. Likewise at lower pHs, the amine groups of CV were protonated and could not be adsorbed on the surface of polyaniline with positive charges. According to Fig.13 the minimum absorption was observed at pH 7, which reveals the maximum adsorption of CV on composite happened in the neutral condition by comparing of the initial CV concentration.

3.6. Mechanism of the adsorption

The surfaces of conducting polyaniline/ hollow $MnFe_2O_4$ nanocomposite are positively charged that vary in forms at different pHs. As the pH of the CV solution reached to basic condition, a proportional decrease in adsorption took place due to the successive deprotonation of on the adsorbent and electrostatic repulsion between electron pair sites of amine groups on the adsorbent and dye's amine electron pairs. There was also competition between OH^- (at high pH) and dye's amines electron pairs for adsorption of positively charged sites on adsorbent.

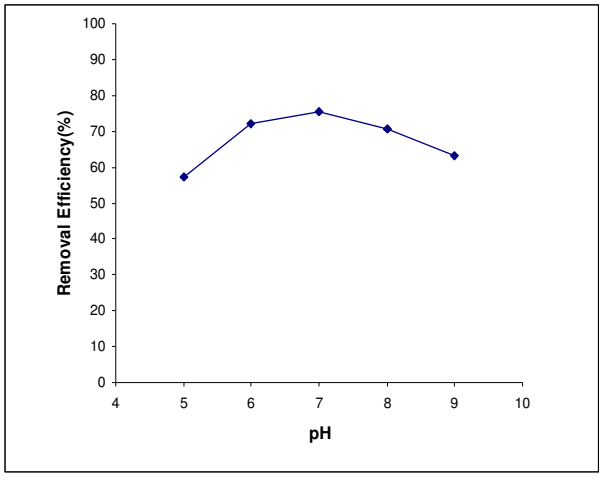

Fig.12. Removal CV in various pHs. Conditions: 0.025 g nanocomposite, 10 ml of 5ppm CV, Agitation time of 15 min.

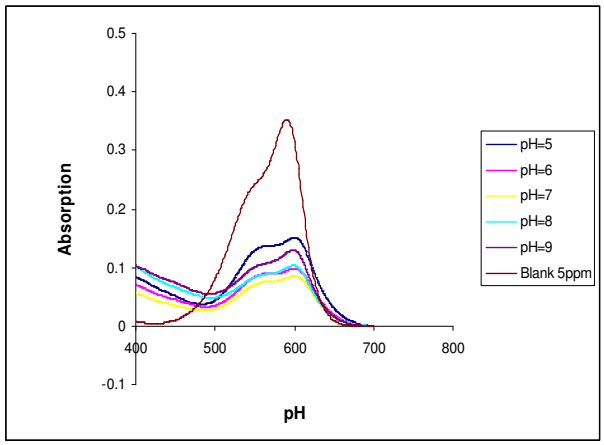

Fig.13. UV-Vis Spectra of CV in various pHs (after and before adsorption). Conditions: 0.025 g nanocomposite, 10 ml of 5ppm CV, Agitation time of 15 min.

3.7. Adsorption behavior in various concentrations

Adsorption studies were carried out with different initial concentrations of CV (1–50 mgL^{-1}) at 25°C and pH 7. As fig.14 and fig.15 show, the percent removal of the CV dye with raise of solution concentration increased, which the maximum adsorption was at the 50 ppm CV. Also, these peaks obviously show that the curve gradient grows at 1-20 ppm much sharper than 20-50 ppm does. Therefore 0.05 g of the nanocomposite was approximately saturated at 20 ppm of the solution.

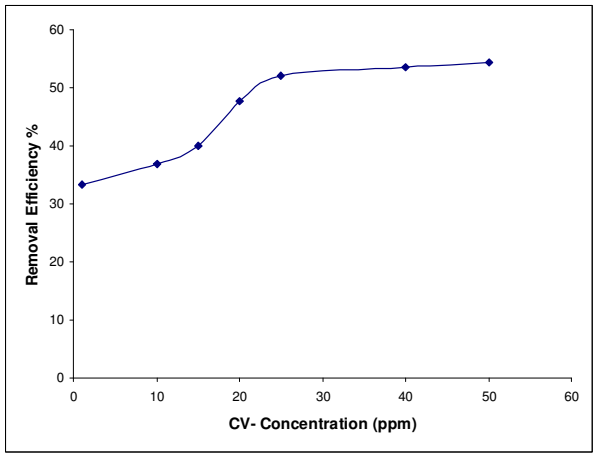

Fig.14. Removal of CV in various concentrations. Conditions: 0.05 g nanocomposite, 50 ml of 1-50 ppm CV solutions, Agitation time of 15 min.

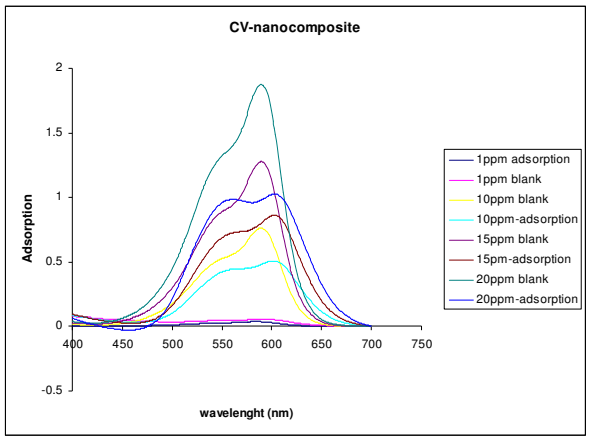

Fig.15. UV-Vis spectra of different concentrations CV (after and before adsorption on nanocomposite) amount of adsorbent is 0.05 g and pH of the solutions is 7.

4. Conclusion

In summary, the PANI/ $MnFe_2O_4$ nanocomposite containing hollow ferromagnetic nanoparticles has been synthesized. This report is a helpful method to improve mixability of inorganic particles with an organic phase. The results of AFM image indicate the even distribution of $MnFe_2O_4$ in the PANI base and this proves the effectiveness of DBSA and ultrasonic devices in mixing two nonhomogenious phases. UV spectra display that the prepared naoncomposite has a suitable ability to remove the group of textile dyes with the similar structure to CV containing amine groups at the ends of dye molecules. As 75.6 % of 5 ppm CV solution (10 ml) was adsorbed by mentioned nanocompoiste, removal efficiency might be increased by using of more weights adsorbent in the proportional volumes of various concentrations.

References

[1] J. Stejskal, R.G. Gilbert, Polyaniline Preparation of a Conducting Polymer, ***Pure Appl. Chem***. 74 (2002) 857-867.

[2] J.E. Albuquerque, L.H.C. Mattoso, D.T. Balogh, R.M. Faria, J.G. Masters, A.G. Mac Diarmid, A simple method to estimate the oxidation state of polyanilines, ***Synth. Met.*** 113 (2000) 19-22.

[3] B. Lesiak, A. Jablonski, J. Zemek, M. Trchova, "Determination of the Inelastic Mean Free Path of Electrons in Different Polyaniline Samples" ***J. Stejskal, Langmuir*** 16 (2000) 1415-1423.

[4] J. Lei, V.P. Menon, C.R. Martin, ***Polym. Adv.Technol.*** 4 (1992) 124-132.

[5] J.G. Deng, X.B. Ding, Y.X. Peng, Magnetic and conducting Fe3O4 cross-linked polyaniline nanoparticles with core-shell structure, ***Polymer*** 43 (2002) 2179-2184.

[6] J. Zhang, A.L. Barker, D. Mandler, P.R. Unwin, "Effect of Surface Pressure on the Insulator to Metal Transition of a Langmuir Polyaniline Monolayer" ***J. Am. Chem. Soc***. 125 (2003) 9312-9313.

[7] G.V. Kurlyandskaya, J. Cunanan, S.M. Bhagat, J.C. Aphesteguy, S.E. Jacobo, Field-induced microwave absorption in Fe3O4 nanoparticles and Fe3O4/polyaniline composites synthesized by different methods, ***J.Phys. Chem. Solids*** 28 (2007) 1527-1532.

[8] S.K. Pillalamarri, F.D. Blum, A.T. Tokuhiro, M.F. Bertino, One-Pot Synthesis of Polyaniline–Metal Nanocomposites Chem, ***Mater.*** 17 (2005) 5941-5944.

[9] Zhiming Zhang, Meixiang Wan, Nanostructures of polyaniline composites containing nano-magnet ***Synth. Met.*** 132 (2003) 205-212.

[10] Q.L. Yang, J. Zhai, L. Feng, Y.L. Song, M.X. Wan, L. Jiang, W.G. Xu, Q.S. Li, Synthesis and Characterization of Conducting Polyaniline/γ-Fe_2O_3 Magnetic Nanocomposite, ***Synth. Met***. 135–136 (2003) 819.

[11] J. Deng, X. Ding, W. Zhang, Y. Peng, J. Wang, X. Long, P. Li, A.S.C. Chen, Magnetic and conducting Fe3O4–cross-linked polyaniline nanoparticles with core–shell structure, ***Polymer*** 43 (2002) 2179-2184.

[12] E. Jacobo, C. Aphesteguy, R. Lopez Anton, N.N. Schegoleva, G.V. Kurlyandskaya, Influence of the preparation procedure on the properties of polyaniline based magnetic composites, ***European Polymer Journal*** 43 (2007) 1333–1346.

[13] F. Caruso, M. Spasova, A. Susha, M. Giersig, R.A. Caruso, Magnetic Nanocomposite Particles and Hollow Spheres Constructed by a Sequential Layering Approach, ***Chem. Mater***. 13 (2001) 109-116.

[14] Y.H. Zhu, H. Da, X.L. Yang, Y. Hu, Preparation and characterization of core-shell monodispersed magnetic silica microspheres, ***Colloid Surf.***, A 231 (2003) 123-129.

[15] R. Jain, S. Sikarwar, Photocatalytic and adsorption studies on the removal of dye Congo red from wastewater, ***Int. J. Environ. Pollut***. 27 (2006) 158–178.

[16] V.K. Gupta, A. Mittal, L. Krishnan, V. Gajbe, Adsorption kinetics and column operations for the removal and recovery of malachite green from wastewater using bottom ash, Sep. Purif. Technol. 40 (2004) 87–96.

[17] A. Mittal, L. Kurup (Krishnan), V.K. Gupta, Use of waste materials—bottom ash and de-oiled soya, as potential adsorbents for the removal of Amaranth from aqueous solutions, ***J. Hazard. Mater***. 117 (2005) 171–178.

[18] C.L. Yang, J. McGarrahan, Electrochemical coagulation for textile effluent decolorization, ***J. Hazard. Mater.*** 127 (2005) 40–47.

[19] K.E. Noll, G. Vassilios, W.S. Hou, Adsorption Technology for Air and Water Pollution Control, ***Lewis Publishers,*** Chelsea, MI, USA, 1992.

[20] Y. Zhang, Z. Huang, F. Tang, Ferrite hollow spheres with tunable magnetic properties, ***Thin Solid Films*** 515 (2006) 2555–2561
[21] K.G. Neoh, M.Y. Pun, E.T.K. Kang, K.L. Tan, ***Synth. Met***. 73 (1995) 209.

[22] M.X. Wan, M. Li, J.C. Li, Z.X. Liu, ***J. Appl. Polym. Sci***. 53 (1994) 131.